Proceedings of the
International Conference on Mechanical Engineering 2007
(ICME2007) 29- 31 December 2007, Dhaka, Bangladesh

ICME07-TH-31

MIXED CONVECTION IN A SQUARE CAVITY WITH A HEAT-CONDUCTING HORIZONTAL CIRCULAR CYLINDER

M. M. Rahman[1], M. A. Alim[1] and M. A. H. Mamun[2]

[1] Department of Mathematics, BUET
[2]Department of Mechanical Engineering, BUET

ABSTRACT

Combined free and forced convection in a two dimensional square vented cavity with a uniform heat source applied on the right vertical wall is studied numerically. A circular heat conducting horizontal cylinder is placed somewhere within the cavity. The present study simulates a practical system, such as air-cooled electronic equipment with heat conducting components. Importance is placed on the influences of the configurations and physical properties of the cavity. The development mathematical model is governed by the coupled equations of continuity, momentum and energy, and is solved by employing Galerkin finite element method. The computations are carried out for wide ranges of Reynolds number (*Re*) and the buoyancy parameter (*Ri.*) The results indicate that both the heat transfer rate from the heated wall and the dimensionless temperature in the cavity strongly depend on the configurations of the system studied, such as size, location and thermal conductivity of the cylinder . Detailed results of the interaction between forced airstreams and the buoyancy-driven flow by the heat source are demonstrated by the distributions of the isotherms, streamlines, and the heat transfer coefficient.

Keywords: Heat transfer, finite element method, mixed convection, heat conducting horizontal circular cylinder, square cavity.

1. INTRODUCTION

The studies of buoyancy driven flow characteristics in cavities have received considerable attention in recent years due to its importance in several thermal engineering problems, such as in the design of solar collector, energy conservation, ventilation of buildings, electronic cooling etc. Many authors have recently studied heat transfer in enclosures with partitions, thereby altering the convection flow phenomenon.

Omri and Nasrallah [1] performed numerical analysis by a control volume finite element method on mixed convection in a cavity where inlet and outlet channels were fixed diagonally ascending or descending order. Fluid was injected at lower temperature than the initial temperature of the cavity. They noticed that for $Ri = 0.1$ to 10 and $Re = 10$ to 100, the average temperature at the exit was higher in the descending mode and air injected from the bottom of the hot wall was more effective the removal of heat. Later on, Singh and Sharif [2] extended their works by considering six placement configurations of the inlet and outlet of a differentially heated rectangular enclosure whereas the previous work was limited to only two different configurations of inlet and outlet. Recently, a numerical analysis of laminar mixed convection in an open cavity with a heated wall bounded by a horizontally insulated plate was presented by Manca et al. [3], where they were considered three heating modes: assisting flow, opposing flow and heating from below, and the results were reported for Richardson number from 0.1 to 100, Reynolds numbers from 100 to 1000, and aspect ratio in the range 0.1–1.5. It was shown that the maximum temperature values decrease as the Reynolds and the Richardson numbers increase. The effect of the ratio of channel height to the cavity height was found to play a significant role on streamline and isotherm patterns for different heating configurations. The investigation also indicated that opposing forced flow configuration has the highest thermal performance, in terms of both maximum temperature and average Nusselt number. Later, similar problem for the case of assisting forced flow configuration was tested experimentally by Manca et al. [4] and based on the flow visualization results, they pointed out that for $Re = 1000$ there were two nearly distinct fluid motions: a parallel forced flow in the channel and a recirculation flow inside the cavity and for $Re = 100$ the effect of a stronger buoyancy determined a penetration of thermal plume from the heated plate wall into the upper channel. Very recently Rahman et al. [5] studied numerically the opposing mixed convection in a vented enclosure. They found that with the increase of Reynolds and Richardson numbers the convective heat transfer becomes predominant over the conduction heat transfer and the rate of heat transfer from the heated wall is significantly depended on the position of the inlet port.

However, many authors have recently studied heat

transfer in enclosures with heat-conducting body obstruction, thereby varying the convection flow phenomenon. Shuja et al. [6] investigated the effect of exit port locations and aspect ratio of the heat generating body on the heat transfer characteristics and irreversibility generation in a square cavity. They found that the overall normalized Nusselt number as well as irreversibility was strongly affected by both of the location of exit port and aspect ratios. Papanicolaou and Jaluria [7] studied mixed convection from an isolated heat sources in a rectangular enclosure. Later on, Papanicolaou and Jaluria [8] performed computations on mixed convection from a localized heat source in a cavity with conducting walls and two openings for application of electronic equipment cooling. Hsu et al. [9] numerically investigated mixed convection in a partially divided rectangular enclosure. They considered the divider as a baffle inside the enclosure with two different orientations and indicated that the average Nusselt number and the dimensionless surface temperature dependent on the locations and height of the baffle. Ha et al. [10] considered the problem of natural convection in a horizontal enclosure with a square body. Natural convection in a horizontal layer of fluid with a periodic array of square cylinder in the interior were conducted by Lee et al [11], in which they concluded that the transition of the flow from quasi-steady up to unsteady convection depends on the presence of bodies and aspect ratio effect of the cell. However, in the previous literature a body considered as a rigid wall but was not calculated. In order to calculate interior body, few numerical studies have conducted for couple of decades. One of the systematic numerical investigations of this problem was conducted by House et al. [12], who considered natural convection in a vertical square cavity with heat conducting body, placed on center in order to understand the effect of the heat conducting body on the heat transfer process in the cavity. They showed that for given *Ra* and *Pr*, an existence of conducting body with thermal conductivity ratio less than unity makes heat transfer enhanced.

The purpose of this study is to examine the effect of a heat conducting cylinder on mixed convection in a square cavity. Numerical solutions are obtained over a wide range of Richardson numbers, Reynolds number, and various physical parameters. The dependence of the thermal and flow fields on the sizes and locations of the heat conducting cylinder is studied in detail.

2. MODEL SPECIFICATION

The geometry for the configurations is shown in Fig. 1. The model considered here is a square cavity with a uniform constant heat flux q, applied on the right vertical wall and an inflow opening located on the left vertical wall is arranged at $h_i = 0.2$, whereas the out flow opening at the top of the opposite heated wall and the size of the inlet port is the same size as the exit port which is equal to $w = 0.1L$. (See [5] for details) The cavity has dimensions of $L \times L$ and thus fixing the aspect ratio equal to 1. The other side walls including top and bottom of the cavity are assumed to be adiabatic. It is assumed that the incoming flow is at a uniform velocity, u_i and at the ambient temperature, θ_i. Since the boundary conditions at the exit of the cavities are unknown, values of u, v and θ are extrapolated at each iteration step. The conducting horizontal cylinder is solid with thermal conductivity. The effect of various orientations and size of the conducting cylinder on the heat transport process are studied in the present work.

3. MATHEMATICAL FORMULATION

The flow within the cavity is assumed to be two-dimensional, steady, laminar, incompressible and the fluid properties are to be constant. The radiation effects are taken as negligible and the Boussinesq approximation is used. The dimensionless equations describing the flow are as follows:

$$\frac{\partial U}{\partial X} + \frac{\partial V}{\partial Y} = 0 \tag{1}$$

$$\mathrm{U}\frac{\partial \mathrm{U}}{\partial \mathrm{X}} + \mathrm{V}\frac{\partial \mathrm{U}}{\partial \mathrm{Y}} = -\frac{\partial \mathrm{P}}{\partial \mathrm{X}} + \frac{1}{\mathrm{Re}}\left(\frac{\partial^2 \mathrm{U}}{\partial \mathrm{X}^2} + \frac{\partial^2 \mathrm{U}}{\partial \mathrm{Y}^2}\right) \tag{2}$$

$$U\frac{\partial V}{\partial X} + V\frac{\partial V}{\partial Y} = -\frac{\partial P}{\partial Y} + \frac{1}{\mathrm{Re}}\left(\frac{\partial^2 V}{\partial X^2} + \frac{\partial^2 V}{\partial Y^2}\right) + RiT \tag{3}$$

$$U\frac{\partial T}{\partial X} + V\frac{\partial T}{\partial Y} = \frac{1}{\mathrm{RePr}}\left(\frac{\partial^2 T}{\partial X^2} + \frac{\partial^2 T}{\partial Y^2}\right) \tag{4}$$

For solid cylinder the energy equation is

$$0 = \frac{K}{\mathrm{RePr}}\left(\frac{\partial^2 T_S}{\partial X^2} + \frac{\partial^2 T_S}{\partial Y^2}\right) \tag{5}$$

Here K is the ratio of the thermal conductivity of the cylinder to that of the fluid, $\mathrm{Gr} = \dfrac{\beta \mathrm{gqL}^4}{\upsilon^2 k}$ is the Grashof number, $\mathrm{Pr} = \dfrac{\upsilon}{\alpha}$ is the Prandtl number, $\mathrm{Re} = \dfrac{\mathrm{u_i L}}{\upsilon}$ is the Reynolds number and $\mathrm{Ri} = \dfrac{\mathrm{Gr}}{\mathrm{Re}^2}$ is the Richardson number.

The above equations were non dimensionalized by defining

$$X = \frac{x}{L},\ Y = \frac{y}{L},\ U = \frac{u}{u_i},\ V = \frac{v}{u_i},\ P = \frac{p}{\rho u_i{}^2},$$

$$T = \frac{k_f(\theta - \theta_i)}{qL},\ T_S = \frac{k_S(\theta_S - \theta_i)}{qL}$$

Where X and Y are the coordinates varying along horizontal and vertical directions, respectively, U and V are, the velocity components in the X and Y directions, respectively, T is the dimensionless temperature and P is the dimensionless pressure.

The boundary conditions for the present problem are specified as follows:

At the Inlet: $U = 1$, $V = 0$, $T = 0$

At the outlet: Convective boundary condition (CBC), $P = 0$

At all solid boundaries: $U = 0, V = 0$

At the heated right vertical wall: $\frac{\partial T}{\partial X} = -1$

At the left, top and bottom walls: $\frac{\partial T}{\partial N} = 0$

At the fluid-solid interface: $\left(\frac{\partial T}{\partial N}\right)_{fluid} = K\left(\frac{\partial T_S}{\partial N}\right)_{solid}$

Where N is the non-dimensional distances either X or Y direction acting normal to the surface and K is the dimensionless ratio of the thermal conductivity $\left(K_S / K_f\right)$

The average Nusselt number at the heated wall has calculated as

$Nu = \frac{1}{L_H}\int_0^{L_H} \frac{h(y).y}{k} dy$ and the bulk average temperature has defined as $T_{av} = \int T\, d\overline{V} / \overline{V}$

where L_H, $h(y)$ are the length and the local convection heat transfer coefficient of the heated wall respectively and $\overline{V}$ is the cavity volume, which should be minimized.

4. COMPUTATIONAL PROCEDURE

The numerical procedure used in this work is based on the Galerkin weighted residual method of finite element formulation. The approximation functions used in the Galerkin method are required to be of higher order. The governing equations has been linearized and solved by segregated solution method. The conjugate residual scheme is used to solve the symmetric pressure type equation systems, while the conjugate gradient squared is used for the non-symmetric advection diffusion type equations. The matrix factorization technique (LU decomposition) is used with partial pivoting. Interpolation function is used to the entire element and expresses the variation of the field variable inside the element in terms of the global axes which are defined for the entire domain or body.

Geometry studied in this paper is an obstructed cavity; therefore several grid size sensitivity tests were conducted in this geometry to determine the sufficiency of the mesh scheme and to ensure that the solutions are grid independent. This is obtained when numerical results of the average Nusselt number *Nu*, average temperature *Tav* and solution time become grid size independent, although we continue the refinement of the mesh grid. As can be seen in Table 1, five different non-uniform grids with the following number of nodes and elements were considered for the grid refinement tests: 24545 nodes, 3788 elements; 29321 nodes, 5900 elements; 37787 nodes, 5900 elements; 38163 nodes, 5962 elements and 48030 nodes, 7516 elements. As is shown in Table 1, 38163 nodes and 5962 elements can be chosen throughout the simulation to optimize the relation between the accuracy required and the computing time.

The present code was extensively exercised on problem [12] to check its validity. We recall here some results obtained by our code in comparison with those reported in [12] for Ra = 0.0, 10^5 and two values of K = 0.2 and 5.0. Table 2 compares the present results with the results by House et al. [12]. The present results have an excellent agreement with the results obtained by House et al. [12].

5. RESULTS AND DISCUSSION

It is necessary to examine the range of the governing parameters *Re* and *Ri* chosen in the present study. In order to maintain laminar flow in the cavity, the values of *Re* and *Ri* are considered in the ranges 50 to 200 and 0 to 10 respectively. Although we have considered the thermal conductivity ratio K equal to 0.2, 1.0, 5.0, and 10.0, emphasis is placed on results for a thermal conductivity ratio K = 5.0. Physically, this value of K represents a solid cylinder of wood in a gas with properties similar to those of air. The Prandtl number throughout the current study is set to 0.71 in accordance with the work of House et al. [12]. Some representative results are shown in figures 2-6 in terms of streamlines and isotherms.

We first show the effects of the heat-conducting cylinder on the flow and thermal fields in the cavity. Streamlines and isotherms plots for without cylinder and with cylinder of various diameter are shown respectively in Figs. 2a (i-iv) and 2b (i-iv) while K = 5.0, Re = 100, Ri = 1.0 and Pr = 0.71. From Fig. 2a (i), it can be seen that two different sizes recirculating cells have developed at the upper and lower side of the inlet port location in the cavity. As compared the Fig. 2a (i) with the Figs. 2a (ii-iv), the solid cylinder in the enclosure consequently reduces the strength of the circulating cell induced by the heat source. In Fig. 2a (ii), which is for cylinder of diameter D = 0.1, only small differences in streamlines have observed when compared with Fig. 2a (i). The fact that a small size of solid cylinder has little significant influence on the convective flow in the enclosure. In addition, increasing the size of the cylinder gives rise to decrease in the space available for the buoyancy-induced recirculating flow. Figs. 2b (i-iv) show the contours of dimensionless temperature (T) for without cylinder and with cylinder of diameter D = 0.1, D = 0.2, and D = 0.5 respectively, while K = 5.0, Re = 100, Ri = 1.0 and Pr = 0.71. It can be seen that isothermal lines are vertically parallel to each other and concentrated around the heated wall, which is similar to conduction-like distribution. Some deviation of isothermal lines is observed for the case of without cylinder. The effect of the heat-conducting cylinder on the average Nusselt number and average temperature is depicted in Fig. 7. It is seen that the values of average Nusselt number increases and average temperature decreases as cylinder diameter increases it size.

Now looking into Figs. 3a (i-iv), that are for K = 0.2, 1.0, 5.0 and 10.0 while Re = 100, Ri = 1.0, D =0.2 and Pr = 0.71, it can be seen that two different sizes recirculating cells developed at the near of the inlet position. We may further observe that streamlines are almost identical for those cases. The effect of thermal conductivity ratio on the isotherms is shown in the Figs. 3b (i-iv). From these figs. it can be seen easily that for increasing values of the thermal conductivity ratio, the isothermal lines moves away from the centre of the heat conducting cylinder. On

the other hand in Fig. 8, we see that the average Nusselt number decreases as the thermal conductivity ratio increases and the lower average temperature is observed at lower thermal conductivity ratio.

The effect of the parameter *Re* on the thermal and flow fields is shown in Fig. 4. For a small value of *Re* (*Re* = 50), the thermal transport effect by the external cold air is little. This is why two small secondary recirculating cells are confined at the upper and lower side of the inlet port. However, as the value of *Re* increases, both the recirculating cells are enhanced and occupy almost the half of the cavity displayed in Figs. 4a (i-iv). As noted, at *Re* = 200, another small vortex of very low speed is developed by the pocket of fluid trapped at the corner of the cavity. The corresponding temperature distributions can be seen in Figs. 4b (i-iv). It can be seen that increase in *Re* reduces the thermal boundary layer thickness and it is possible, since at larger value of *Re,* the effect of gravitation force becomes negligible. The effect of the Reynolds number *Re* on the average Nusselt number and average temperature is shown in Fig. 8. It is noteworthy that the values of average Nusselt number increases and average temperature decreases as *Re* increases, which is expected.

Fig. 5 shows streamlines and isotherms for *Ri* = 0.0, 2.5, 5.0 and 10.0, while *Re* = 100, *K* = 5.0, *D* =0.2 and *Pr* = 0.71. For *Ri* = 0.0, only forced convection present and major flow is through diagonally from the inlet to the exit and two relatively small non uniform recirculating cells have formed, located near the upper and lower side at the inlet shown in Fig. 5a (i). In the present of buoyancy effect, i.e. for *Ri* = 2.5 the upper recirculating cell has become relatively large and higher strength and another small vortex of very low speed is developed by the pocket of fluid trapped at the near of the top wall of the cavity shown in Fig. 5a (ii). With the increase in Richardson number i.e. at higher *Ri* (5.0 and 10.0), the pocket of fluid merges with the upper recirculating cell and the cell spreads out inside the cavity and squeezing the induced forced flow shown in 5a (iii-iv).Thermal field is governed more or less by interaction between incoming cold fluid stream and the circulating vortex. It also depends on where the vortex is created inside the cavity. For *Ri* = 0.0, the high temperature region is more concentrated near the hot wall and the temperature distribution is more uniform in the remaining parts of the cavity. On the other hand, the temperature decreases near the hot wall as the value of *Ri* increases shown in Figs. 5b (i-iv).

Finally, the effect of the solid cylinder location on the thermo-fluid fields is shown in Fig. 6. Streamlines and Isothermal lines for various cylinder locations are depicted respectively in Figs. 6a (i-iv) and Figs. 6b (i-iv) while *K* = 5.0, *Re* = 100, *Ri* = 1.0, *D* = 0.2 and *Pr* = 0.71 are keeping fixed. As the solid cylinder is closure to the inlet port along the lower quartile horizontal plane shown in the Figs. 6a (i) and 6b (i), the main-through flow accelerated in the jet direction and a small recirculating cell is formed under the inlet position. Thereby, major portion of heat is carried out by the forced convection and vertically parallel isotherms generate at the heat source. If the cylinder is considered near the left wall along the mid-horizontal plane shown in the Figs. 6a (ii) and 6b (ii), the recirculating cells are confined to occupy the left portion in the cavity and the isothermal lines are almost same as in the previous. Farther the cylinder is considered near the heated (right) wall along the mid-horizontal plane and upper quartile-horizontal plane shown in the Figs. 6a (iii-iv) and 6b (iii-iv). In both cases, streamlines and isotherms are almost same. The variation of the average Nusselt number and average temperature with the locations of the cylinder is shown in Fig. 9.

6. CONCLUSION

The present numerical investigation is made of mixed convection in an enclosure with a heat-conducting horizontal circular cylinder. Results are obtained for wide ranges of parameters *Re* and *Ri,* as well as various configurations of the solid cylinder.

The following conclusions may be drawn from the present investigations

- The average Nusselt number for an enclosure is significantly increased and the average temperature decreases as the cylinder diameter is increased.
- An unexpected result is found for the thermal conductivity ratio. The effect of the small cylinder on heat transfer are negligible, but for large cylinder an obvious enhancement in the heat transfer is observed and the heat transfer rate decreases as the thermal conductivity ratio increases.
- The average Nusselt number for an enclosure is significantly increased and the average temperature decreases as *Re* is increased.
- The value of the average Nusselt number is greater if the location of the cylinder is near the left wall along the mid-horizontal plane or near the heated (right) wall along upper quartile-horizontal plane.

7. ACKNOWLEDGEMENT

The authors like to express their gratitude to the Department of Mathematics, Bangladesh University of Engineering and Technology, Bangladesh for providing computer facility during this work.

8. REFERENCES

1. Omri, A. and Nasrallah, S. B., 1990, “Control Volume Finite Element Numerical Simulation of Mixed Convection in an Air-Cooled Cavity”, Numerical Heat Transfer, Part A, 18: 213–225.
2. Singh, S. and Sharif, M. A. R., 2003, “Mixed Convection Cooling of a Rectangular Cavity with Inlet and Exit Openings on Differentially Heated Side Walls”, Numerical Heat Transfer, Part A, 44: 233–253.
3. Manca, O., Nardini, S., Khanafer, K. and Vafai, K., 2003, “Effect of Heated Wall Position on Mixed Convection in a Channel with an Open Cavity”, Experimental Heat Transfer, 43: 259–282.
4. Manca, O., Nardini, S. and Vafai, K., 2006, “Experimental investigation of Mixed Convection in

a Channel with an Open Cavity", Numerical Heat Transfer, Part A, 19: 53–68.
5. Rahman, M.M., Alim, M.A.,Mamun, M.A.H., Chowdhury, M.K. and Islam, A.K.M.S., 2007, "Numerical Study of Opposing Mixed Convection in a Vented Enclosure", ARPN Journal of Engineering and Applied Sciences, 2(2): 25-36.
6. Shuja, S. Z., Yilbas, B. S. and Iqbal, M.O., 2000, "Mixed Convection in a Square Cavity due to Heat Generating Rectangular Body Effect of Cavity Exit Port Locations", Int. J. of Numerical Methods for Heat and Fluid flow, 10 (8): 824–841.
7. Papanicolaou, E. and Jaluria, Y., 1990, "Mixed Convection from an Isolated Heat Source in a Rectangular Enclosure", Numerical Heat Transfer, Part A, 18: 427–461.
8. Papanicolaou, E. and Jaluria, Y., 1993, "Mixed Convection from a Localized Heat Source in a Cavity with Conducting Walls: A Numerical Study", Numerical Heat Transfer, Part A, 23: 463–484.
9. Hsu, T.H., Hsu, P.T. and How, S.P., 1997, "Mixed Convection in a Partially Divided Rectangular Enclosure", Numerical Heat Transfer, Part A, 31: 655-683.
10. Lee, J. R., Ha, M. Y. Balachandar, S. Yoon, H.S. and Lee, S.S., 2004, "Natural Convection in a Horizontal Layer of Fluid with a Periodic Array of Square Cylinders in the Interior", Phys. Fluids, 16: 1097-1117.
11. Ha, M. Y. Yoon, H.S, Yoon, K.S, Balachandar, S., Kim, I, Lee, J.R. Chun, H.H., 2002, "Two-dimensional and unsteady natural convection in a horizontal enclosure with a square body" Numerical Heat Transfer A 41,183–210.
12. House, J. M., Beckermann, C. and Smith, T. F., 1990, "Effect of a Centered Conducting Body on Natural Convection Heat Transfer in an Enclosure", Numerical Heat Transfer, Part A, 18: 213–225.

Table 1: Grid Sensitivity Check at Re = 100, Ri = 1.0 and Pr = 0.71

Nodes (elements)	24545 (3788)	29321 (4556)	37787 (5900)	38163 (5962)	48030 (7516)
Nu	1.91228	1.91244	1.91254	1.91255	1.91259
T_{av}	0.04351	0.04351	0.04351	0.04351	0.04351
Time(sec)	323.610	408.859	563.203	588.390	793.125

Table 2: Nusselt Number Comparison for Pr = 0.71

Ra	k	Nu		
		Present work	House et al. [12]	Error (%)
0	0.2	0.7071	0.7063	0.11
0	1.0	1.0000	1.0000	0.00
0	5.0	1.4142	1.4125	0.12
10^5	0.2	4.6237	4.6239	0.00
10^5	1.0	4.5037	4.5061	0.00
10^5	5.0	4.3190	4.3249	0.14

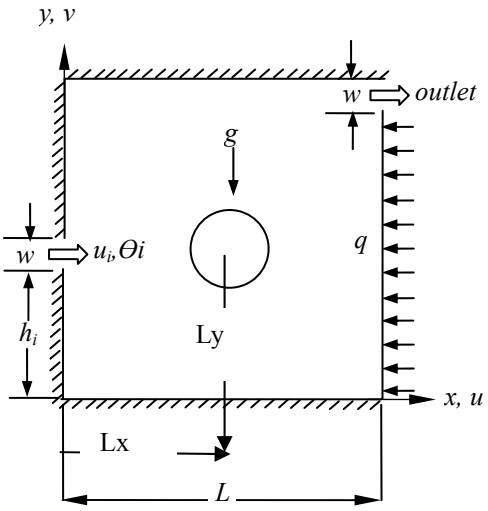

Fig 1: Schematic diagram of the problem considered and coordinate system

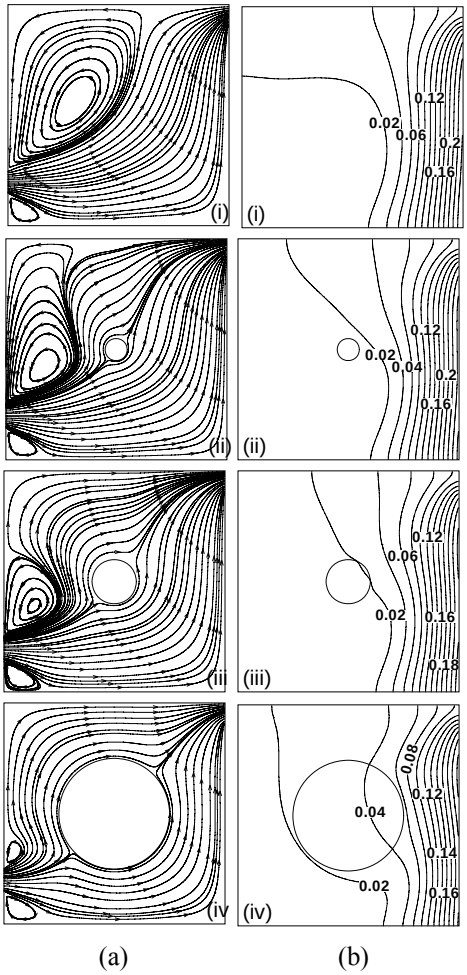

(a) (b)

Fig 2: (a) streamlines and (b) isotherms for (i) without cylinder, (ii) D/L= 0.1, (iii) D/L= 0.2 and (iv) D/L= 0.5, while Re = 100, Ri = 1.0, k = 5.0.

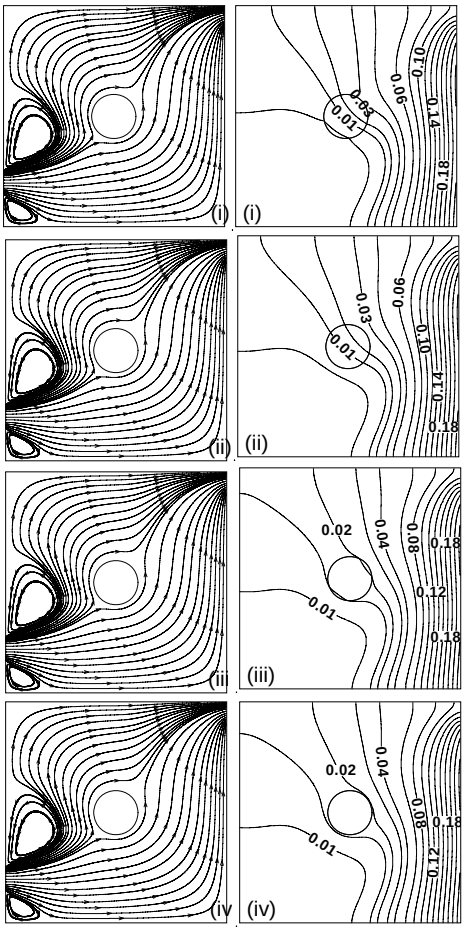

(a) (b)

Fig 3: (a) streamlines and (b) isotherms for (i) k = 0.2, (ii) k = 1.0, (iii) k= 5.0, and (iv) k = 10.0, while Re = 100, Ri = 1.0, D/L = 0.2

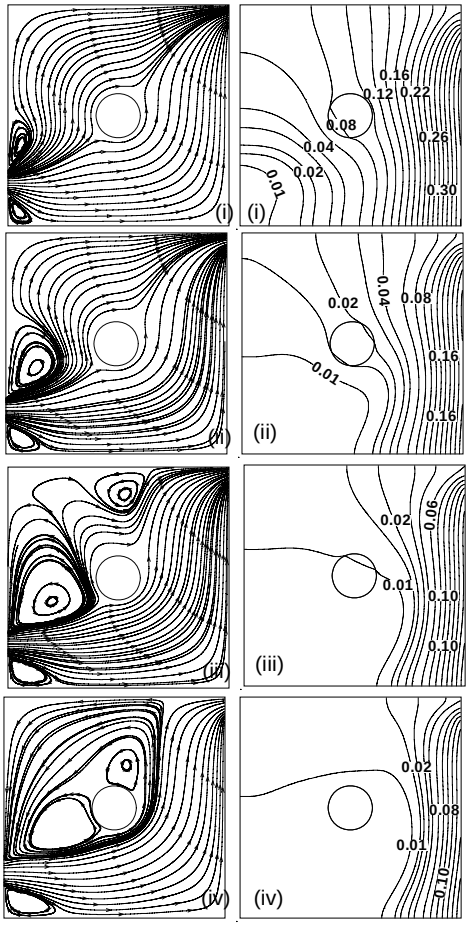

(a) (b)

Fig 4: (a) streamlines and (b) isotherms for (i) Re = 50, (ii) Re = 100, (iii) Re= 150, and (iv) Re = 200, while k = 5, Ri = 1.0, D/L = 0.2.

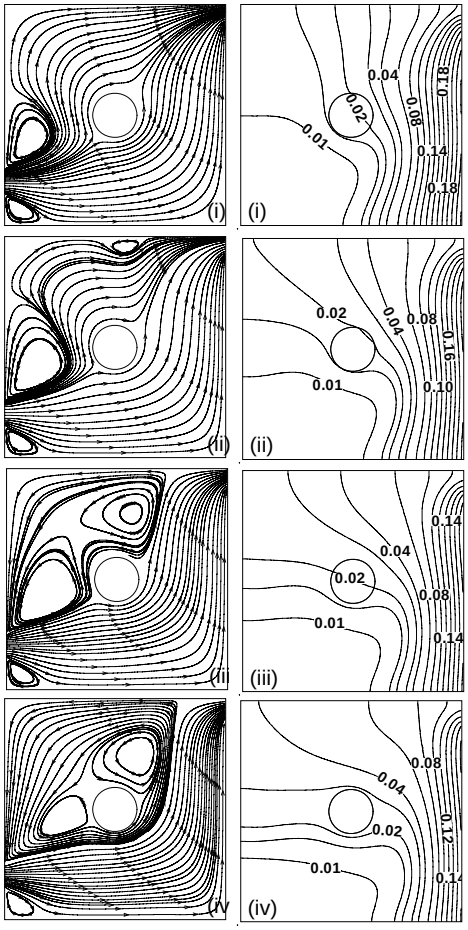

(a) (b)

Fig 5: (a) streamlines and (b) isotherms for (i) Ri = 0.0, (ii) Ri = 2.5, (iii) Ri = 5.0, and (iv) Ri = 10.0, while k = 5, Re = 100, D/L = 0.2

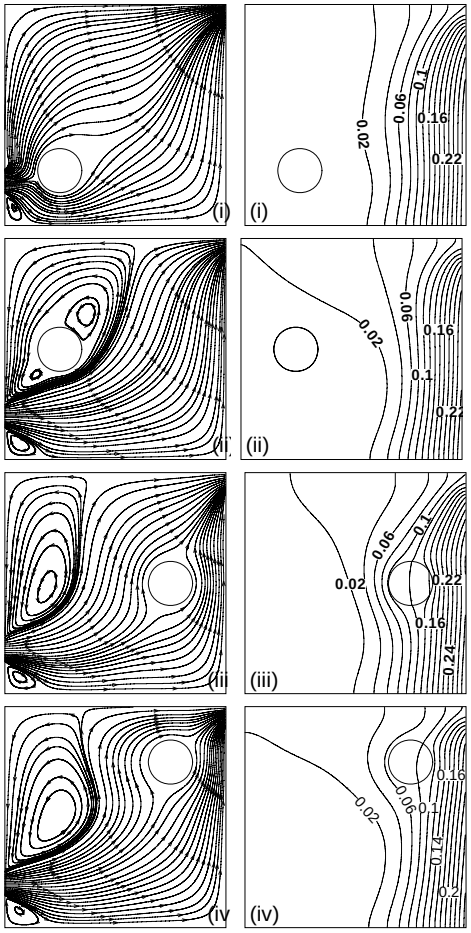

(a) (b)

Fig 6: (a) streamlines and (b) isotherms for (i) Lx /L = Ly / L = 0.25, (ii). Lx /L= 0.75, Ly/L = 0.5 (iii) Lx /L= 0.25, Ly/L = 0.5 and (iv) Lx /L = Ly / L = 0.75, while Re = 100, Ri = 1.0, k = 5.0, D/L = 0.2.

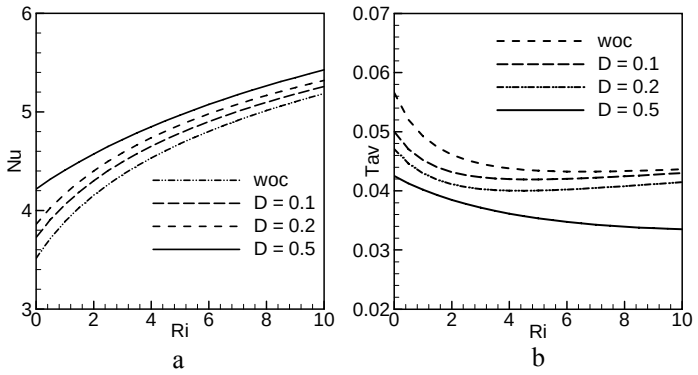

a b

Fig 7: Effect of the cylinder configurations on average Nusselt number and average temperature

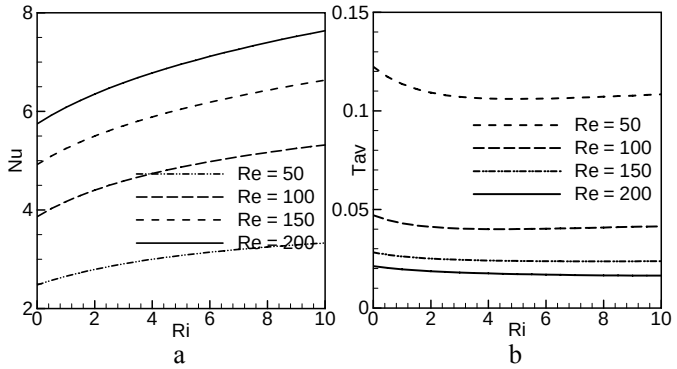

a b

Fig 8: Effect of the Reynolds number on average Nusselt number and average temperature

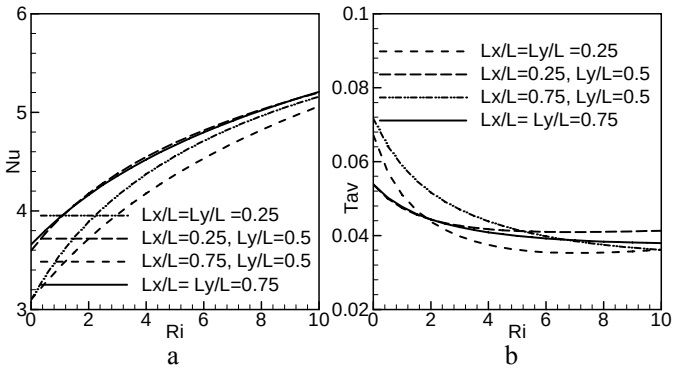

a b

Fig 9: Effect of the cylinder locations on average Nusselt number and average temperature.